Articles

In Situ Fourier Transform Infrared Characterization of the Effect of Electrical Fields on the Flame Synthesis of TiO_2 Particles

Philip W. Morrison, Jr.,* Ram Raghavan, and Andrew J. Timpone

Department of Chemical Engineering, Case Western Reserve University, Cleveland, Ohio 44106-7217

Christian P. Artelt and Sotiris E. Pratsinis

Department of Chemical Engineering, University of Cincinnati, Cincinnati, Ohio 45221-0171

Received September 27, 1996. Revised Manuscript Received September 15, 1997[⊗]

Electric fields facilitate flame synthesis of powders with precisely controlled size and composition. Fourier transform infrared (FTIR) spectroscopy is used for the first time to measure the effect of electric fields on the process temperature and composition during synthesis of titania powders by $TiCl_4$ oxidation in a premixed methane−oxygen flame; flat electrodes apply a dc electric field to the flame. Emission and transmission FTIR spectra are taken at various flame heights. At each height, the FTIR measurements reveal that the particles and the gas have the same temperature. Electric fields modestly increase the flame temperature. The FTIR measured mole fractions of HCl are in good agreement with a mass balance indicating that all $TiCl_4$ is converted to TiO_2 by either direct hydrolysis or oxidation followed by hydrolysis of Cl_2. The absorption spectrum of the TiO_2 indicates that the particles scatter like a collection of ellipsoids. In the absence of electric fields, the particle mass concentration decreases by 20% from 0.3 to 1.3 cm above the burner by gas dilution. In the presence of electric fields, however, that concentration decreases by 70% over the same distance. Thus, FTIR spectroscopy is a powerful diagnostic tool that can provide in situ information of the temperature, composition, and particle characteristics in the adverse environment of electrically modified flames.

Introduction

Though TiO_2 synthesis by $TiCl_4$ oxidation is an established industrial process bringing sizable profits to the corresponding corporations, its fundamentals are not yet well understood. The reason for this stems from the fact that the chemical reaction and particle growth take place very quickly at typical process conditions. These short residence times coupled with the high process temperatures makes it difficult to collect representative samples for particle characterization and model development. This lack of understanding largely limits process control and the manufacturing development of titania and other ceramic particles of closely controlled size, including nanoparticles. Clearly there is a need for on-line diagnostics for understanding and controlling the process.

In situ Fourier transform infrared (FTIR) spectroscopy can provide valuable information about the $TiCl_4$ oxidation process using a combination of emission and transmission measurements (E/T). The transmission measurements yield information on the gas-phase composition as well as the particle composition, mass fraction, and size; the emission measurements contain information on the temperatures of gases and particles.[1,2] Both gas-phase and particle measurements are available simultaneously. Previous researchers have applied the E/T FTIR technique to gas streams containing silica, ash, and coal particles[3] as well as an ethylene diffusion flame[4] and a coal flame.[5] In flame measurements, tomographic reconstruction of E/T spectra yields the spatial variations of particle and gas compositions.[6−9] In addition, more recent work has been performed on

[⊗] Abstract published in *Advance ACS Abstracts,* November 15, 1997.

(1) Best, P. E.; Carangelo, R. M.; Markham, J. R.; Solomon, P. R. *Combust. Flame* **1986**, *66*, 47.
(2) Solomon, P. R.; Best, P. E. In *Combustion Measurements*; Chigier, N., Ed.; Hemisphere Publishing Corp.: New York, 1991; p 385.
(3) Solomon, P. R.; Carangelo, R. M.; Best, P. E.; Markham, J. R.; Hamblen, D. G. *Fuel* **1987**, *66*, 897.
(4) Solomon, P. R.; Best, P. E.; Carangelo, R. M.; Markham, J. R.; Chien, P. L. In *Twenty-First Symposium (International) on Combustion*; The Combustion Institute: Pittsburgh, PA, 1986; p 1763.
(5) Solomon, P. R.; Chien, P. L.; Carangelo, R. M.; Best, P. E.; Markham, J. R. In *Twenty Second Symposium (International) on Combustion*; The Combustion Institute: Pittsburgh, PA, 1988; p 211.
(6) Best, P. E.; Chien, P. L.; Carangelo, R. M.; Solomon, P. R. *Combust. Flame* **1991**, *85*, 309.
(7) Markham, J. R.; Zhang, Y. P.; Carangelo, R. M.; Solomon, P. R. In *Twenty-third Symposium (International) on Combustion*; The Combustion Institute: Pittsburgh, PA, 1990; p 1869.
(8) Morrison, P. W., Jr., Cosgrove, J. E.; Markham, J. R.; Solomon, P. R. In *MRS International Conference Proceedings Series: New Diamond Science and Technology (Proceedings of the Second International Conference on New Diamond Science and Technology*; Messier, R., Glass, J. T., Butler, J. E., Roy, R., Eds.; Materials Research Society: Pittsburgh, PA, 1991; p 219.

S0897-4756(96)00508-X CCC: $14.00

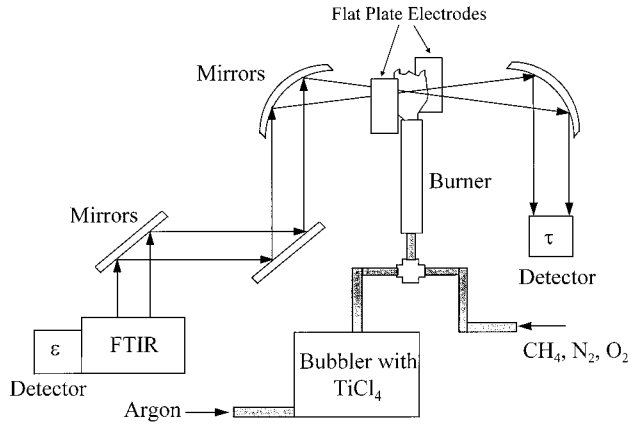

Figure 1. Schematic diagram of the FTIR system as coupled to the burner. The transmission detector is marked τ while the emission detector is marked ϵ. The vertical height of the IR beam is controlled by moving the position of the burner.

fume particles found in a commercial black liquor recover boiler.[10]

The goal of this study is to show that in situ Fourier transform infrared (FTIR) spectroscopy can be used to unravel the dynamics of the concurrent chemical kinetics and aerosol dynamics during titania synthesis in a simple reactor scheme: $TiCl_4$ oxidation in a premixed flame. Similar flame reactors are routinely used for manufacture of TiO_2 at a rate of 100 tons/day.[11] In situ IR measurements are particularly useful when titania particles are made in the presence of electric fields which are employed for synthesis of precisely sized nanoparticles.[12] At these conditions, even the process temperature cannot be measured by conventional means (e.g., thermocouples). In addition, in situ FTIR can reveal the evolution of chemical species and provide insight on the fundamentals of the early process stages. The results below show that in situ E/T FTIR can quantitatively measure the temperature and gas composition of premixed TiO_2 flames. In addition, one can also determine the TiO_2 particle temperature and relative concentration.

Experimental Section

Burner. Figure 1 shows a schematic of the experimental setup.[13] A laminar premixed, burner-stabilized flame reactor is used to make titania particles in the presence of an electric field across the flame. The flame is stabilized on the burner mouth using a 2 cm long mullite monolith (Corning) honeycomb with 48 openings/cm^2. To provide good mixing of the reactants before they enter the honeycomb, the burner (alumina tube (Coors), 1.875 cm i.d.) is packed to three-quarters of its length with glass beads (6 mm in diameter) supported on a screen. The advantage of using a burner-stabilized, premixed, flat flame is that most of the particles experience similar temperatures and gas velocities across the flame.[14]

Clean, dry argon gas (Wright Brothers, 99.8%) is bubbled into the gas washing bottle containing $TiCl_4$ (Aldrich, 99.9%) and premixed with particle-free nitrogen (Wright Brothers, 99.8%), oxygen (Matheson, 99.9%), and methane (Wright Brothers, 99.8%) and sent through the burner. The flow rates of the gases are Ar = 300 sccm, N_2 = 3300 sccm, O_2 = 1000 sccm, and CH_4 = 500 sccm. A check valve is used before the precursor is mixed with the mixture of air and methane so as to prevent any back flow of the flame. Oxide particles are formed in the flame by oxidation/hydrolysis of the precursors.

Stainless steel, plate electrodes (3.8 × 2.5 × 0.38 cm) are used to create the electric field across the flame.[13] One electrode is connected to a d.c power supply (Gamma High Voltage Research, Inc.) with reversible polarity, and the second is connected to ground. The distance between the plates is 5 cm, and they are arranged in such a way as the plate bottoms are 2 mm above the burner face. The applied field intensities are 0, −1.5, and −2 kV/cm.

FTIR Spectrometer and Optics. The FTIR spectrometer is a Bomem MB157 operating over the spectral range 6500−500 cm^{-1} with a resolution of 4 cm^{-1}. For the measurements discussed below, the spectrometer uses a wide-band deuterated triglycine sulfate (DTGS) detector for the transmission measurements and a HgCdTe detector for the emission measurements. The transmission detector is mounted opposite the spectrometer on the far side of the flame while the emission detector is attached directly to the MB157 (Figure 1). Two off-axis paraboloidal mirrors focus the IR through the flame; the spot size of the FTIR beam is less than 1 cm^2. Emission and transmission measurements take place directly through the flame at three different positions: the lower edge of the IR beam is 0.3, 0.8, or 1.3 cm above the burner tip. The vertical height of the IR beam is controlled by setting the position of the burner prior to an experiment.

The path correction spectrum for the emission measurements is taken using a blackbody cavity in place of the burner while the background spectrum for the transmission is taken with the burner off.[15] The optical path between the spectrometer and the detectors is not purged, so the single-beam spectra for all the FTIR measurements contain absorptions due to the atmospheric CO_2 and H_2O. However, since the path correction and the background spectrum are taken with the same optical path, most of the effects of the atmospheric CO_2 and H_2O are removed when the emittance (emission single beam/path correction) and the transmittance (transmission single beam/background) are calculated. This procedure does not remove all of the atmospheric absorptions in the spectra because the background concentrations of CO_2 and H_2O drift over time, but these concentration changes are very small compared to the large concentrations of CO_2 and H_2O found in the flame. Typically we collect 20 scans of the transmission spectra followed by turning off the IR source in the spectrometer and then collecting 50 scans of the emission spectrum. Spectra are taken at one flame height at all electric field intensities before changing the burner height.

Theory

Transmission Measurements of Particles and Gases. The analysis of the E/T data follows the procedures outlined in Best et al.[1,2,10] The transmittance spectra yield concentration information for the gases and particles while the combination of radiance (emission) and transmittance spectra determine gas and particle temperatures. A brief outline of the procedures is given here.

In general, the absorbance spectrum ($A(\nu)$) of a collection of gases and particles is defined as[1,2,10]

$$A(\nu) = -\log \tau(\nu) = (k(\nu)cL + \sum_i N_i C_{\mathrm{ext},i}(\nu)L)/2.303 \quad (1)$$

(9) Bates, S. C.; Carangelo, R. M.; Knight, K.; Serio, M. A. *Rev. Sci. Instrum.* **1993**, *64*, 1213.
(10) Morrison, P. W., Jr., Cosgrove, J. E.; Carangelo, R. M.; Carangelo, M. D.; Solomon, P. R.; Leroueil, P.; Thorn, P. A. *TAPPI J.* **1991**, *74*, 68.
(11) Stamatakis, P.; Natalie, C. A.; Palmer, B. R.; Yuill, W. A. *Aerosol Sci. Technol.* **1991**, *14*, 316.
(12) Vemury, S.; Pratsinis, S. E. *Appl. Phys. Lett.* **1995**, *66*, 3275.
(13) Vemury, S.; Pratsinis, S. E. *J. Aerosol Sci.* **1996**, *27*, 951.
(14) Vijayakumar, R.; Whitby, K. T. *Aerosol Sci. Technol.* **1984**, *3*, 17.
(15) Morrison, P. W., Jr. Haigis, J. R. *J. Vac. Sci. Technol. A* **1993**, *11*, 490.

where ν = wavenumber (cm^{-1}), $\tau(\nu)$ = transmittance, $k(\nu)$ = absorptivity for the gas (cm^2/mol), c = concentration of the gas (mol/cm^3), N_i = number density of the ith particle size (number/cm^3 of gas), $C_{ext,i}(\nu)$ = extinction cross section for the ith particle size (cm^2), and L = path length through the sample stream. The first term accounts for gas absorption while the second term is the result of particle absorption and scattering. The parameters $k(\nu)$ and $C_{ext,i}(\nu)$ are independent of c and N_i at the low values of concentration and number density in the flames under consideration. The major difference between the two is that gas absorption bands are sharply peaked within a spectral region a few hundred wavenumbers wide, while $C_{ext,i}(\nu)$ varies smoothly across large regions of the spectrum. The combination of the gases and particles produces a spectrum with gas absorption peaks superimposed upon a nonzero baseline resulting from particle extinction; simple baseline subtraction can isolate the two effects.

Emission/Transmission FTIR. The normalized radiance ($R_n(\nu)$) yields temperature information and is defined as the ratio $R(\nu)/[1 - \tau(\nu)]$ where $R(\nu)$ = sample radiance. The normalized radiance of a hot sample stream surrounded by cold walls relates to gas and particle temperatures as follows:[2]

$$R_n(\nu) = \frac{R(\nu)}{1 - \tau(\nu)} = \frac{k(\nu)c\ BB(\nu,T_g) + \sum N_i C_{abs,i}\ BB(\nu,T_p)}{k(\nu)c + \sum N_i C_{ext,i}} \quad (2)$$

$$C_{ext} = C_{abs} + C_{sca} \quad (3)$$

where $BB(\nu,T)$ = the Planck spectral function for a blackbody at temperature T (W/sr m^2 cm^{-1}), T_g = gas temperature, T_p = particle temperature, C_{abs} = absorption cross section of a particle, and C_{sca} = scattering cross section of a particle. The expression for the Planck spectral function is given by[16]

$$BB(\nu,T) = \frac{C_1 \nu^3}{\exp(C_2\nu/T) - 1} \quad (4)$$

where $C_1 = 1.191 \times 10^{-8}$ W/sr m^2 $(cm^{-1})^4$ and $C_2 = 1.439$ cm K. When the gas stream contains no particles ($N_i = 0$), eq 2 predicts that the normalized radiance is identical with $BB(\nu,T_g)$ wherever $k(\nu)$ is not zero. For regions of the spectrum where the gas is not absorbing ($k(\nu) = 0$) and particle absorption dominates the extinction ($C_{ext} \approx C_{abs}$), then $R_n(\nu) = BB(\nu,T_p)$. In the case where the sample contains both particles and gases, one can correct the transmittance and radiance to remove the particle contributions. Calculating the normalized radiance from the corrected spectra yields the gas temperature as if there were the no particles present.

It is important to realize that eqs 1−2 are averages along the IR beam. For the purposes of this research, this is an acceptable approximation since the distribution of temperatures and gas velocities is fairly uniform across the premixed flame.[14] In principle, however, one can perform a series of E/T FTIR measurements across a nonuniform process stream and then tomographically reconstruct the data to produce point values for transmittance and radiance.[6−8]

Rayleigh Extinction by Submicron Particles. Given the submicron size of the particles and the wavelength range (2−20 μm), we can employ Rayleigh extinction theory to calculate $C_{ext,i}(\nu)$.[17] Rayleigh theory strictly applies to spherical particles although one may extend it to encompass generalized ellipsoids (including spheres, disks, and needles), cubes, or a continuous distribution of ellipsoids.[17] Thus, one can calculate the cross sections for absorption and scattering using the following equations:[17]

$$C_{abs,i} = k\ \mathrm{Im}\ \alpha(\nu,V_i) \quad (5)$$

$$C_{sca,i} = (k^4/6\pi)|\alpha(\nu,V_i)|^2 \quad (6)$$

where $k = 2\pi n_m \nu$, n_m = index of refraction of the gas matrix = 1, $\alpha(\nu,V_i)$ = polarizability of a particle of size i, and V_i = volume of a particle of size i. Im signifies the imaginary part of the complex expression.

The expression for the polarizability $\alpha(\nu,V_i)$ depends on the dielectric function $\epsilon(\nu)$, the volume of the particles V_i, and the shape of the particles.[17] In all cases, $\alpha(\nu,V_i)$ has the form

$$\alpha(\nu,V_i) = V_i\, f(\epsilon(\nu)) \quad (7)$$

where $\epsilon(\nu)$ = complex dielectric function of the TiO_2 particles. Thus, as long as the shape of the particles do not change, $C_{abs,i}$ is proportional to V_i, and the particle absorption is proportional to the total volume of particles $\Sigma N_i V_i$ in the IR beam (eqs 5 and 7). Furthermore, in spectral regions where absorption ≫ scattering ($C_{sca} \approx 0$ and $C_{ext} \approx C_{abs}$), $A(\nu)$ varies directly with the total mass of particles in the IR beam (eq 1); for titania, this occurs at wavenumbers < 1000 cm^{-1}.

In principle calculation of C_{ext} is possible given the dielectric function for TiO_2 and an assumption for the shape of the particles. Currently there are several obstacles that prevent accurate calculation of C_{ext}. First, flame synthesis of titania produces mostly the anatase phase,[12,18] and the optical constants of anatase TiO_2 are not currently available. Second, the particles are highly agglomerated, and choosing a shape distribution is problematic at this point in time. Preliminary calculations of C_{ext} using the optical constants of rutile TiO_2[19] indicate that the shape of the measured spectra is not consistent with spherical particles but more closely resembles a continuous distribution of ellipsoidal shapes (CDE).[17,20] (An example of the CDE calculation appears in Figure 2a). The predicted magnitude of the calculated spectra is incorrect, however. This discrepancy is most likely due to the agglomeration of the primary particles into clusters whose extinction properties are not captured in the above calculations. Nonetheless, we can still calculate the relative amounts of

(16) Griffiths, P. R.; de Haseth, J. A. *Fourier Transform Infrared Spectrometry*; John Wiley and Sons: New York, 1986.

(17) Bohren, C. F.; Huffman, D. R. *Absorption and Scattering of Light by Small Particles*; John Wiley and Sons: New York, 1983.

(18) Pratsinis, S. E.; Zhu, W.; Vemury, S. *Powder Technol.* **1996**, *86*, 87.

(19) Ribarsky, M. W. In *Handbook of Optical Constants of Solids*; Palik, E. D., Ed.; Academic Press: Orlando, FL, 1985; Vol. 1, p 795.

(20) Huffman, D. R.; Bohren, C. F. In *Light Scattering by Irregularly Shaped Particles*; Schuerman, D., Ed. Plenum: New York, 1980; p 103.

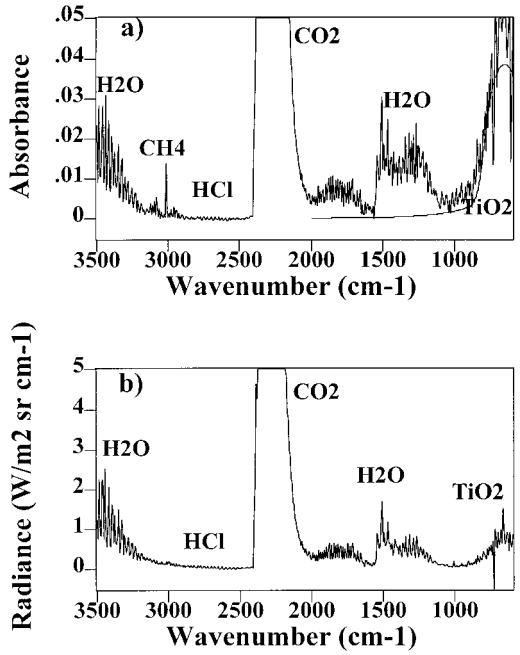

Figure 2. In situ FTIR spectra of the premixed flame TiO_2 flame taken 0.3 cm above the burner tip with no electric field. (a) Absorbance spectrum calculated from the transmittance measurement; also shown is a calculated spectrum for TiO_2 particles assuming a continuous distribution of ellipsoidal shapes. (b) Radiance (emission) spectrum of flame.

TiO_2 in the flame by comparing the relative magnitude of the TiO_2 absorption feature.

Results and Discussion

Figure 2 shows the FTIR spectra of a premixed CH_4/O_2 flame producing TiO_2 particles by $TiCl_4$ oxidation in the absence of electric fields; the measurement position is 0.3 cm above the burner face. The absorbance spectra of the flames contain the dominant features of CO_2 and H_2O and the minor features of CH_4 and HCl (Figure 2a). There is no observable CO in the flame, which indicates that the combustion process goes to completion. In the spectral region near 500 cm^{-1}, $TiCl_4$ also is not observed because the large amount of H_2O in the spectrum overwhelms any absorption produced by the small amount of $TiCl_4$ (<0.06%) in the flame. The spectra also show a broad absorbance between 600 and 800 cm^{-1} due to absorption by the TiO_2 particles. At high wavenumbers where scattering is strongest, there is actually very little extinction by particle scattering. This is consistent with the fact that the particle size and concentration are very small.[12,13] This observation also precludes the presence of any soot in the flame since soot would absorb strongly at high wavenumbers.[1,4]

Temperature Analysis. The absorbance spectrum in Figure 2a is calculated from the transmittance $\tau(\nu)$ and thus is related to the $[1 - \tau(\nu)]$ spectrum; Figure 2b shows the corresponding radiance spectrum. Note that the spectral features are the same except for the CH_4 absorption in the transmission spectrum. This observation leads to the conclusion that the CH_4 is cold (no radiance) compared to the other hot gases and the TiO_2 particles. Cold CH_4 would result if there were a CH_4 leak of some sort into the ambient surrounding the flame.

If the particle and gas temperatures were equal to each other, we can simplify eq 2 using $T_g = T_p = T$ and

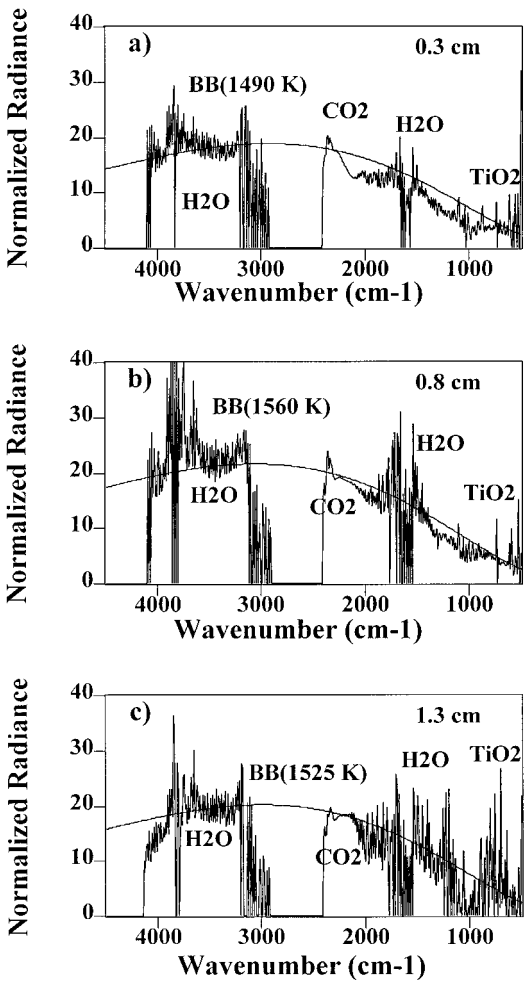

Figure 3. Normalized radiance spectra ($R(\nu)/[1 - \tau(\nu)]$) at zero electric field. Spectra are shown for various positions above the burner: (a) 0.3, (b) 0.8, and (c) 1.3 cm; also shown are Planck functions (blackbody) spectra (smooth line envelopes) that match the normalized radiance. Data corresponding to values of $[1 - \tau(\nu)] < 0.005$ are omitted for clarity.

noting that $C_{ext} \approx C_{abs}$ since the particle scattering is small throughout the spectrum. With these simplifications, one finds that

$$R_n(\nu) = BB(\nu,T) \qquad \text{if } T_p = T_g \tag{8}$$

Thus we can determine the temperature of the flame by comparing the normalized radiance to Planck functions at various temperatures until a good match is achieved. The normalized FTIR radiance spectra at three heights above the burner are shown in the absence (Figure 3) and presence of an applied field of −2 kV/cm (Figure 4). Portions of the spectra where $[1 - \tau(\nu)]$ is less than 0.005 are omitted for clarity. The calculated Planck functions also appear in Figures 3 and 4, and the temperature results are further summarized in Table 1.

There are several general features to note from the spectra in Figures 3 and 4. In an ideal situation where all the gases and particles have exactly the same temperature, the normalized radiance would lie on the Planck curve wherever the gases and particles have absorption features. By and large this is true for each of the major species: H_2O (4000−3300, 2000−1200, and near 500 cm^{-1}), CO_2 (2400−2000 cm^{-1}), and TiO_2 (800−500 cm^{-1}). The only exception is the CH_4 band near

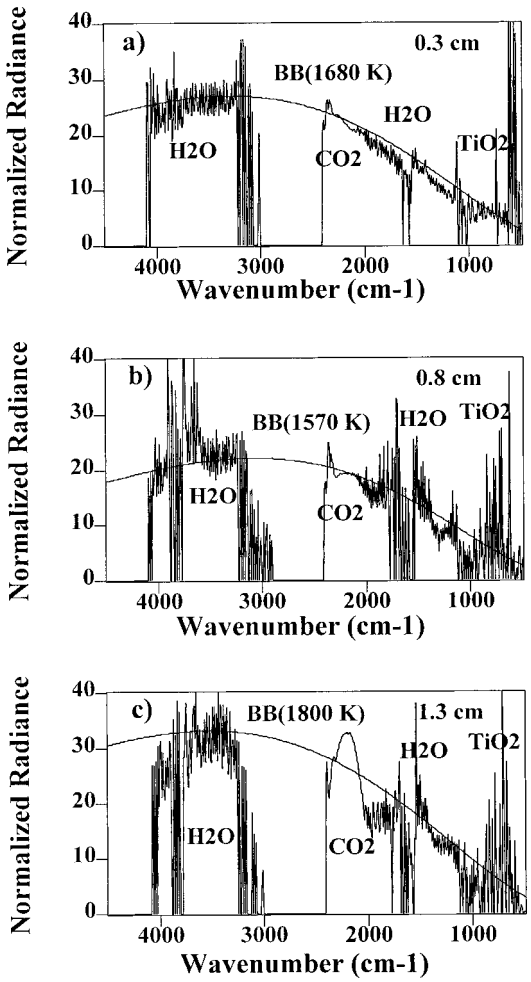

Figure 4. Normalized radiance spectra ($R(\nu)/[1 - \tau(\nu)]$) at a field of −2 kV/cm. Spectra are shown for various positions above the burner: (a) 0.3, (b) 0.8, and (c) 1.3 cm; also shown are Planck functions (blackbody) spectra (smooth line envelopes) that match the normalized radiance. Data corresponding to values of $[1 - \tau(\nu)] < 0.005$ are omitted for clarity.

3000 cm^{-1}. These results confirm the assumption that $T_p = T_g$. Please note that the portion of $R_n(\nu)$ at high wavenumbers (e.g., the H_2O band at 4000−3300 cm^{-1}) is a sensitive measure of temperature, so obtaining a match between $R_n(\nu)$ and the Planck function throughout the spectrum attests to the quality of the fit.

Within an individual gas band, however, there are often some deviations from the Planck curve which indicates that the gas has some variations in its temperature across the flame. In the case of CO_2 (2350 cm^{-1}), these deviations are the most easily observed because of the low noise. In the flame with zero field (Figure 3a), the CO_2 band at 0.3 cm shows some significant departures from the Planck function shown, and these departures become much smaller at 0.8 cm (Figure 3b) and 1.3 cm (Figure 3c). The deviations in Figure 3 amount to a maximum of ∼200 K for Figure 3a and maximum of ∼75 K in Figure 3b,c. Thus, the radial temperature distribution in the flame (no field) is broader near the burner than farther down stream. In the flame with an electric field (Figure 4), the opposite is true: the radial temperature distribution is most uniform near the burner (0.3 cm) and least uniform at 1.3 cm. Again the nonuniformities amount to ∼50 K for Figure 4a,b and ∼200 K for Figure 4c. These observations emphasize the fact that the E/T method is a line-of-sight technique which will yield an average temperature unless tomographic techniques are employed.[6−9] In many cases, however, the flame is radially homogeneous.

The noise observed in the normalized radiance is primarily due to the noise in the transmittance spectrum and is generally largest where the absorption features are the smallest. The noise is least in the CO_2 band because of the large absorption and emission signals in the transmittance and radiance spectra (Figure 2). Conversely, the noise in the H_2O and TiO_2 portions of the spectrum is significantly higher (see Figure 2a). The noise at low wavenumbers increases with flame height due to increasing velocity fluctuations at the tip of the flame (Figure 3). Such velocity fluctuations cause flickering in the FTIR signal which is picked up as noise by the spectrometer.

Gas Analysis. Once the temperature of the flame is known, quantitative determination of the gas concentrations is possible by calculating the actual FTIR absorbance spectrum of a gas given the temperature and total pressure as well as the partial pressure and spectroscopic constants of the gas.[21,22] This calculation procedure systematically accounts for any deviations from Beer's law caused by the limited resolution in the FTIR spectrometer.[23] The spectroscopic constants for CH_4, HCl, CO_2, and H_2O are found in the HITRAN database.[24,25] A sample of the results of such absorbance calculations for HCl, CO_2, and H_2O appears in Figure 5 using the partial pressures shown. In the case of CO_2 and H_2O, the partial pressures of 0.1 and 0.2 atm are chosen based on a mass balance around the flame. The partial pressure for the HCl is varied until a good fit is achieved. The calculations for CH_4 match the measured spectra best if one assumes a temperature of 300 K, thus supporting the suspicions that a methane leak is present. Subsequent evaluation of the burner indicated a fine fracture that would have caused CH_4 to escape prior to reaching the flame front. Table 1 contains a summary for all conditions along with error estimates.

In general, the calculated spectra match the measured spectra in both amplitude and shape. The major exception is the CO_2 spectrum, which shows a poor fit below 2300 cm^{-1}. The cause for this is missing data in the HITRAN database which become important at temperatures above 1000 K. The presence of HCl in the flame arises either from the direct hydrolysis of $TiCl_4$ to TiO_2 or via the oxidation of $TiCl_4$ followed by the hydrolysis of the Cl_2 byproduct. In either event, we expect that the chlorine entering with the $TiCl_4$ to appear in the flame as HCl. Note that Cl_2 has no absorptions in the IR, so if some of the Cl_2 escapes hydrolysis, we would find that the FTIR measurements could not close the

(21) Taweechokesupsin, O. In situ Gas Phase Measurements Using Infrared Spectroscopy During Hot Filament Chemical Vapor Deposition of Diamond. M.S. Thesis, Case Western Reserve University, Cleveland, OH, 1996.
(22) Morrison, P. W., Jr. Taweechokesupsin, O. *J. Quantum Spectrosc. Radiat. Transfer*, submitted.
(23) Anderson, R. J.; Griffiths, P. R. *Anal. Chem*. **1975**, *47*, 2339.
(24) Rothman, L. S.; Gamache, R.; Goldman, A.; Brown, L.; Toth, R.; Pickett, H.; Poynter, R.; Flaud, J.; Camy-Peyret, C.; Barbe, A.; Husson, N.; Rinsland, C.; Smith, M. *Appl. Opt*. **1987**, *26*, 4058.
(25) Rothman, L.; Gamache, R.; Tipping, R.; Rinsland, C.; Smith, M.; Benner, D.; Malathy Devi, V.; Flaud, J. M.; Camy-Peyret, C.; Perrin, A.; Goldman, A.; Massie, S.; Brown, L.; Toth, R. *J. Quantum Spectrosc. Radiat. Transfer* **1992**, *48*, 469.

Table 1. Summary Results of in Situ FTIR Measurements on a Premixed TiO_2 Flame[a]

electric field (kV/cm)	position (cm)	temp (K) (±100 K)	relative TiO_2 concn (±0.1)	P_{CO_2} (atm) (±0.01)	P_{H_2O} (atm) (±0.02)	P_{HCl} (atm) (±0.001)	P_{CH_4} (atm)
0	0.3	1490	1.0	0.1	0.2	0.003	0.0015
	0.8	1560	1.0	0.1	0.2	0.0025	0.0015
	1.3	1525	0.8	0.1	0.2	0.0025	0.001
−1.5	0.3	1540	0.9	0.1	0.2	0.0025	0.0005
	0.8	1550	0.8	0.1	0.2	0.0025	0.0015
	1.3	1800 (max = 2000)	0.5	0.1	0.2	0.0025	0.001
−2	0.3	1680	0.9	0.1	0.2	0.003	0.0005
	0.8	1570	0.7	0.1	0.2	0.0025	0.002
	1.3	1800 (max = 2000)	0.3	0.1	0.2	0.0025	0.00025

[a] The position is the distance above the burner. The TiO_2 particles and the gases are all at the temperatures quoted above; the only exception is CH_4 which has a temperature of 300 K in all cases. The absolute temperature errors are ± 100 K while the relative temperature errors are ± 50 K.

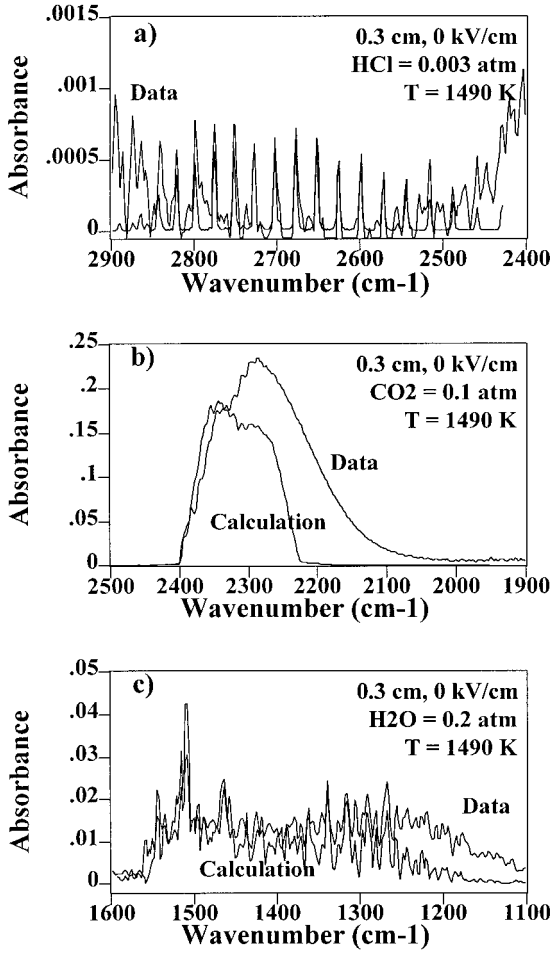

Figure 5. Calculated absorbance spectra of HCl, CO_2, and H_2O in a CH_4/O_2 flame at zero electric field and 0.3 cm above the burner. (a) HCl at a partial pressure of 0.003 atm, (b) CO_2 at a partial pressure of 0.1 atm, and (c) H_2O at a partial pressure of 0.2 atm. The calculated absorbance spectra use the measured gas temperature of 1490 K (Figure 3a).

chlorine mass balance because some of the incoming chlorine would "disappear" as Cl_2. Weighing the bubbler over a period of 6 h of operation, we calculate the molar flow rate of $TiCl_4$ into the flame as 1.28×10^{-4} mol/min which corresponds to a mole fraction of ~0.053%. (The measured molar flow rate is 88% of the value calculated using the $TiCl_4$ vapor pressure data found in Knacke et al.[26]). Assuming that all the chlorine in $TiCl_4$ is hydrolyzed to form HCl, the mole fraction of HCl in the flame should be 0.22% or a partial pressure of 0.0022 atm. This is in excellent agreement with the measured partial pressures of (0.0025−0.003) ± 0.001 atm.

Particle Analysis. As mentioned previously, the shape of the TiO_2 feature (Figure 2a) indicates that the particles do not behave optically as spheres but more like a randomly oriented distribution of randomly shaped ellipsoids. Other authors have reached similar conclusions with SiC particles[17] and quartz particles.[20] A likely cause for this observation is the agglomeration of primary particles into randomly shaped clusters that scatter and absorb as if they were ellipsoids.[12]

More detailed quantitative analysis of the TiO_2 spectra is not possible because we lack the optical constants of anatase TiO_2 and the shape distribution of the particles. Nonetheless, because the particle absorption is proportional to the mass of particles in the beam, measuring the amount of TiO_2 absorption between 800 and 600 cm^{-1} will yield the relative amount of TiO_2 mass in the IR beam. This analysis is valid as long as (1) the optical constants of the TiO_2 do not change significantly with temperature and (2) the particle shapes do not change appreciably. In general, the complex dielectric function of a metal oxide is roughly constant over a temperature change of 300−500 K.[27,28] In addition, relatively large changes in the shape distribution (e.g., sphere vs cube or sphere vs CDE) are required to change $\alpha(\nu,V_i)$ and C_{abs}.[17] Thus, the above approximations appear to be valid for this situation. The results of the relative TiO_2 concentrations appear in Table 1. The results have been normalized so that the concentration at 0.3 cm in the flame without electric fields is equal to one. Using the measured temperature and a mass balance, this concentration corresponds to 0.42 $\mu g/cm^3$. This concentration will vary ~10% depending on the local temperature because of changes in the local volumetric flow of the gases.

Effects of Electric Fields on Temperature and Particle Concentrations. The imposed electric fields have a significant impact on the flame temperatures as shown in Figures 3 and 4 and Table 1. Because of averaging across the line of sight, the measured temperatures listed in Table 1 have an absolute accuracy of ±100 K and a relative accuracy of ±50 K. At zero electric field, the temperature in the flame is approximately 1500 K and is roughly independent of axial position in the flame although there may be a slight

(26) Knacke, O., Kubaschewski, O., Hesselmann, K., Eds.; *Thermochemical Properties of Inorganic Substances*, 2nd ed.; Springer-Verlag: Berlin, 1991; Vol. 1.

(27) Thomas, M. E. *P. Soc. Photo.* **1989**, *1112*, 260.

(28) Thomas, M. E. In *Handbook of Optical Constants of Solids II*, 1st ed.; Palik, E. D., Ed.; Academic Press: Boston, 1991; p 177.

temperature rise at the middle position (Figure 3). The temperature is fairly uniform across the flame except at the lowest position (Figure 3a). At 0.3 cm above the burner, the CO_2 temperature shows a variation of ~200 K; the temperatures of the H_2O and TiO_2, however, are more uniform at 1490 K ± 100 K. In general, the applied electric field tends to increase the flame temperature and the axial temperature gradient. For example, at −1.5 kV/cm, the electric field has little effect on the temperature at the two lowest axial positions, but the temperature increases to roughly 1800 K at the highest position (1.3 cm). For the case of −2 kV/cm, the temperature at the lower positions is ~100−200 K hotter than the flame with no field and at 1.3 cm the difference rises to ~300 K (Figure 4). In addition, the portions of the CO_2 band at 1.3 cm show significantly higher temperatures ranging from the average temperature of 1800 K to a maximum of 2000 K. A likely cause of the inhomogeneity is the visible fluctuations in the tip of the flame when an electric field is applied. All of the above temperatures are well below the adiabatic flame temperature of ~2450 K. Previous investigators have applied electric fields to hydrocarbon flames and performed detailed studies of soot formation,[29] but this is the first time that the temperature of these electrically modified flames has been measured at various axial locations. Incidentally, the results of this study are in qualitative agreement with the modest increase of the temperature by electric discharges.[29] Future FTIR studies using tomographic techniques are planned to elucidate the radial structure of the flame.

The concentrations of the TiO_2 particles are also affected by the imposed electric field, but the gas concentrations are not (Table 1). This is not surprising in light of the fact that the nanoparticles can hold charge. At zero field, the TiO_2, CO_2, and H_2O concentrations do not decrease axially except for a 20% decrease in the TiO_2 concentration at the highest measurement point. The decrease at the upper position is probably due to a slight spreading of the flame. With the electric field on, particle concentrations are ~10% lower at the bottom position and 50−70% lower at the top position; furthermore, the particle concentration decreases as the electric field increases. When electric fields are applied across a the flame, its shape is altered more drastically at the flame top than at the bottom.[29,30] Thus, the FTIR results are consistent with the visual turbulence induced in the flame by the applied field. However, the turbulence is not causing mixing with the atmosphere because the gas concentrations are not diluted. The field could be removing the charged particles from the IR beam by electrophoresis resulting in a decrease in the observed particle concentration. In addition, the inhomogeneity in the radial temperature is greatest at the upper position so that thermophoresis may be important as well. However, one must be careful because two competing processes take place. Electrophoresis sweeps particles out of the flame reducing particle number and mass (yield) concentration (e.g., Figure 10 in Vemury and Pratsinis[13]). At the same time nanoparticles are charged and do not coagulate as fast as in the absence of charges so higher particle number concentrations arise. This second process, however, would not be observed in our measurements since the FTIR is measuring mass concentration, not number concentration.

(29) The Electrochemical Society: Pennington, NJ.

(30) Vemury, S.; Pratsinis, S. E.; Kibbey, L. *J. Mater. Res.* **1996**, *12*, 1031.

Conclusions

The above results demonstrate that emission/transmission FTIR measurements of a premixed TiO_2 flame can yield valuable information. The FTIR measurements can determine the particle temperature and concentrations as well as gas temperatures and concentrations. In most cases, the gas and particle temperatures are the same, and the flame temperature is fairly uniform across the flame width. An applied electric field increases the temperature of the flame: at the lowest measurement position (0.3 cm), the temperature rises from ~1500 to ~1700 K while at the highest measurement position (1.3 cm), it rises form ~1500 to ~1800 K. Transmission measurements show that large amounts of hot CO_2 and H_2O are present while small partial pressures (0.001−0.003 atm) of hot HCl and cold CH_4 are also found. The FTIR measured concentrations are in excellent agreement with a mass balance across the flame. For the first time, FTIR enabled acquisition of in situ temperature measurements during the electrically modified flame synthesis of particles. Furthermore, FTIR quantitatively shows that all the $TiCl_4$ is converted to TiO_2 either by direct hydrolysis or by oxidation followed by hydrolysis of the Cl_2 byproduct.

Using Rayleigh theory, semiquantitative analysis of the particle spectra is possible. These results indicate that the spectral shape of the particle extinction is inconsistent with spherical particles and more consistent with a distribution of ellipsoidal shapes; any analysis of laser light scattering in such flames must take this possibility into account. Although quantitative analysis is not currently possible for these agglomerated particles, relative mass concentrations can be extracted from the FTIR spectra. At the highest measurement position (1.3 cm), the particle concentration decreases ~20% without an electric field, whereas the particle concentration drops by 70% when an electric field is applied. Although the reduction in concentration may have resulted from the coalescence of the TiO_2 agglomerates, detailed microscopic and specific surface area analyses have shown that this is not the case in electrically modified flame synthesis of titania.[12] In addition, since measured partial pressures of the gases do not change with axial distance for any of the flames studied, dilution of the flame with atmospheric air is unlikely. Thus, the applied electric field is preferentially sweeping charged particles out of the flame by electrophoretic forces as well-as enhancing thermophoresis by increasing temperature gradients. The applied field also induces visible turbulence in the flame as well-as additional noise in the IR spectra.

In conclusion, we have shown that FTIR is a powerful diagnostic tool that can provide in situ information on the temperature, composition and particle characteristics in the adverse environment of electrically modified flames.

Acknowledgment. This research has been supported by National Science Foundation grants CTS-9625095 (P.W.M.) and CTS-9612107 (S.E.P.) as well as the Case School of Engineering (P.W.M.).

CM960508U